scientific reports

Check for updates

OPEN

Icariin inhibits proliferation and migration of VSMCs via LncRNA H19 competitively binding to HuR

Yibing Zhang[1], Peng Huang[2], Min Li[3] & Zhimin Fan[4]✉

Developing new anti-atherosclerotic agents and exploring their mechanistic actions is required. This study defined the molecular mechanism of icariin (ICA) in human aortic smooth muscle cells (HA-VSMCs) proliferation and migration by focusing on lncRNA H19 mediated the ability of the HuR protein to bind target mRNAs. The levels of lncRNA H19, cyclin D1 and matrix metalloproteinase-9 (MMP-9) were measured via qPCR or western blot. The 3-(4,5-dimethylthiazol-2-yl)-5-(3-carboxymethoxyphenyl)-2-(4-sulfophenyl)-2 H-tetrazolium (MTS), flow cytometry and transwell assays were performed to determine the functions of lncRNA H19 in cell proliferation and migration. RNA pull down and RIP were performed to verify the interaction between lncRNA H19 and HuR, or interaction between HuR and target mRNAs. LncRNA H19 expression was modulated in response to treatment with ICA. LncRNA H19 overexpression inhibited the proliferation and migration of ox-LDL-induced HA-VSMCs. ICA attenuated cell proliferation and migration, which was reversed by lncRNA H19 knockdown. LncRNA H19 overexpression reduced the expression of cyclin D1/MMP-9, and restrained the stability of cyclin D1/MMP-9 mRNAs. Moreover, lncRNA H19 was found to bind with HuR to decrease the mRNA stability of cyclin D1/MMP-9 mRNAs. In addition, ICA suppressed the expression of cyclin D1/MMP-9, this effect was partly reversed by lncRNA H19 knockdown. We propose that lncRNA H19 serves as an endogenous competing RNA to disable HuR, restricting its availability to target cyclin D1/MMP-9 mRNAs, generally repressing HA-VSMCs proliferation and migration. ICA inhibits proliferation and migration of HA-VSMCs, altering the expression of cyclin D1 and MMP-9, in a lncRNA H19/HuR dependent manner.

Keywords Icariin, LncRNA H19, Human vascular smooth muscle cells, Atherosclerosis, HuR

Atherosclerosis (AS), characterized by progressing atherosclerotic plaques formation and luminal narrowing of arteries, is the principal cause of cardiovascular disease (CVD) with high mortality worldwide[1]. The basic cause of atheroma is the dysfunction of multiple cell types, such as endothelial cells (ECs), macrophages and vascular smooth muscle cells (VSMCs). It has been well defined that the abnormal apoptosis, proliferation and migration of VSMCs are indispensable for AS[2]. Evidence has shown that oxidized low-density lipoprotein (ox-LDL) could be a crucial factor in the genesis of AS via activating monocytes/macrophages, inducing ECs dysfunction, and promoting proliferation and migration of VSMCs[3]. Currently, drugs such as statins are the principal therapies for AS, but the high incidence of AS-related CVD remains a healthcare and economic burden[4]. Hence, developing new therapeutic agents and exploring their mechanistic actions is required to improve AS management.

There is an increasing amount of evidence supporting that some active constituents in traditional Chinese herbal medicine emerge as complementary or alternative options for AS therapy[5,6]. Icariin (ICA) is a bioactive ingredient extracted from *Herba epimedii*, which has the effects of anti-tumor, anti-inflammation, immune regulation, protecting cardiovascular system and so on[7–9]. Our previous study demonstrates that ICA suppresses the progression of AS in apolipoprotein E-deficient ($ApoE^{-/-}$) mice, and ICA represses the proliferation and migration of human aortic smooth muscle cells (HA-VSMCs)[10,11]. Nonetheless, the related mechanisms underlying the role of ICA in AS need further exploration.

Long non-coding RNAs (lncRNAs) have attracted increasing research attention especially with regard to their regulatory action on proliferation and migration of VSMCs in AS[12,13]. Previous work from our lab

[1]Department of Ophthalmology, The First Hospital of Jilin University, Jilin University, Changchun, China. [2]School of Agroforestry and Medicine, The Open University of China, Beijing, China. [3]Department of Experimental Pharmacology and Toxicology, School of Pharmacy, Jilin University, Changchun, China. [4]Department of Breast Surgery, The First Hospital of Jilin University, Jilin University, 71 Xinmin Ave, Changchun 130021, China. ✉email: fanzhimin2023@126.com; fanzm@jlu.edu.cn

utilized microarray analysis to explore the gene expression profiles of ICA-treated ApoE$^{-/-}$ mice[10], and identify upregulated lncRNA H19 (Gene ID: NR_001592) expression upon ICA intervention. LncRNA H19 has been found to correlate with AS[14,15], however, the regulatory mechanisms of lncRNA H19 in AS are largely unknown. LncRNAs can regulate mRNA decay and translation, working corporately with RNA-binding proteins (RBPs) and microRNAs (miRNAs). Human antigen R (HuR) is the ubiquitous member of the Hu/ELAV (human/embryonic lethal abnormal vision) RBP family and is responsible for the stabilization and/or translation of many target mRNAs[16]. Several atherosclerotic regulators involved in various steps in AS are regulated by HuR, including cyclins, matrix metalloproteinases (MMPs), and cytokines[17–19]. More importantly, it has been demonstrated that HuR associates with lncRNA H19 and blocks the processing of miR-675 from lncRNA H19[20].

In this study, we report the regulatory effect of lncRNA H19 on ox-LDL-induced HA-VSMCs, and present evidence that lncRNA H19 overexpression specifically decreases the stability of mRNAs encoding the cyclin D1 and MMP-9. We assess that lncRNA H19 may function as endogenous competing RNAs for HuR, sponging its activity away from target mRNAs. Our results also highlight the function of ICA regulated lncRNA H19 expression, resulting in the suppression of HA-VSMCs proliferation and migration. These findings might provide a new light for the treatment of AS, as well as a novel molecular mechanism of ICA protected AS.

Materials and methods

Bioinformatics analysis

Our lab used microarray analysis to investigate the gene expression profiles of ICA-treated ApoE$^{-/-}$mice in previous work[10]. Based on the lncRNA expression profiling measured by Clariom™ D solutions for Mouse (Affymetrix GeneChip, Santa Clara, CA), the random variance model (RVM) t-test was used to filter differentially expressed lncRNAs for the ICA-treated and model groups. To discern the genes that were differentially expressed, we chose a p value < 0.05 by ANOVA as the threshold screening between the treatment and the model groups.

Cell culture and treatment

HA-VSMCs were purchased from the Chinese Academy of Sciences Cell Bank (Shanghai, China, Cat. No. GNH 46) (Supplementary Fig. S1A-B) and cultured in DMEM/F12 medium (Invitrogen, USA, No. 11330032) supplemented with 10% foetal bovine serum (FBS), 100 mg/ml streptomycin and 100 U/ml penicillin (all from Invitrogen) in a 5% CO_2 atmosphere at 37 °C. The cell line was tested negative for Mycoplasma (MycoAlertTM mycoplasma detection kit, LT07-418, LONZA). This cell line was authenticated by short tandem repeat profiling in LandM Biotechnology (Guangzhou, China).

Ox-LDL was purchased from Yiyuan Biotechnologies (Guangzhou, China, No. YB-002). ICA (molecular weight: 676.67 g/mol, molecular formula: $C_{33}H_{40}O_{15}$) was obtained from Vic's Biotechnologies (Sichuan, China, No. 489-32-7). ICA was dissolved in dimethyl sulfoxide (Sigma-Aldrich, USA, No. D8418) and diluted to 10 μM with the culture medium. Following pretreatment with ICA, cells were treated with 25 μg/ml ox-LDL 30 min later.

Cell proliferation assay

Cell proliferation assay was performed with an MTS assay kit. Briefly, cells after different treatments were suspended and seeded into 96-well plates, after 24, 48 and 72 h. The proliferation of HA-VSMCs was determined by the tetrazolium compound [(3-(4,5-dimethylthiazol-2-yl)−5-(3-carboxymethoxyphenyl)−2-(4-sulfophenyl)−2 H-tetrazolium, inner salt; MTS] reduction method (Promega, USA, Cat. No. G5421) to the manufacturer's procedure. The absorbance of each well was measured at λ = 490 nm using a microplate reader (Thermo Fisher, USA).

Flow cytometry assay

Cell-cycle distribution was determined by measuring the cellular DNA content using flow cytometry. Briefly, 1×10^6 cells were seeded in six-well plates and cultured for 48 h at 37˚C. Next, cells were harvested and stained with propidium iodide (PI) for 30 min at 4˚C after fixing with 70% ethanol for 30 min at 4˚C. Then DNA content of cells was detected on a flow cytometer (Becton Dickinson, USA). The percentages of cells in G0/G1, S and G2/M phases were analyzed with ModFit LT 3.0 software (Variety, USA).

Transwell migration assay

HA-VSMCs were harvested with 100 μl of serum-free medium and plated in the top chamber of transwell (8 μm pore filters; Corning, USA), 600 μl of DMEM/F12 medium containing 10% FBS was placed in the bottom chamber. Then, drugs with corresponding concentrations were placed in the bottom chamber also. After 24 h of incubation, the cells attached to the upper surface of the filter membranes were gently removed with a cotton swab. Migrating cells at the lower surface were fixed with 4% paraformaldehyde, stained with 0.5% crystal violet and photographed using microscope (Olympus, Japan).

Quantitative real-time polymerase chain reaction (qPCR)

Total RNA was extracted from HA-VSMCs. using Trizol reagent (Invitrogen, USA, No. 10296-028), according to the manufacturer's protocols. One μg of RNA per sample was reversely transcribed into cDNA using ImProm-IITM Reverse Transcription System (Promega, USA, No. A3800). Three duplicates with cDNA and SYBR GREEN qPCR Super Mix (Invitrogen, USA, No. C11733046) were conducted in ABI 7500 Fast real-time PCR system (Applied Biosystems, USA). Reversed transcription was performed at 37 °C for 15 min, and cDNA was amplified for 40 cycles: 95 °C for 10 s, 58 °C for 20 s, and 72 °C for 10 s. The GAPDH was used as internal control for lncRNA and mRNA quantification. Results were calculated using $^{\Delta\Delta}$Ct method to determine the

fold change in expression between the experimental and control groups. As shown in Table 1, the forward and reverse primers were synthesized by Sangon Biotech (China).

Cell transfection with SiRNA and plasmids

The small interference RNA (siRNA) against lncRNA H19 and a scramble siRNA as negative control were purchased from Ribobio Biotechnology (Guangzhou, China). The lncRNA H19 siRNA1 target sequence is 5′-CCTCTAGCTTGGAAATGAA-3′, lncRNA H19 siRNA2 5'-GACGTGAGAAGCAGGACAT-3'. To overexpress lncRNA H19, a plasmid vector expressing full-length H19 (2348 bp) was constructed by LandM Biotechnology (Guangzhou, China) and named pLVX-H19 while the empty vector pLVX-IREs-Neo served as negative control. Electrophoresis and sequencing were then performed. HA-VSMCs (2×10^6cells/well) were transfected with Lipofectamine 2000™ (Invitrogen, USA, Cat. No. 11668019) transfection reagent or lipofectamine™ RNAi Max (Invitrogen, USA, Cat. No. 31985070) according to the manufacturer's instructions[21–23]. qPCR was performed after 24 h of transfection to verify the transfection efficiency.

Western blot assay

Total protein samples were separated with 10% SDS-polyacrylamide gels and electrotransferred to polyvinylidene fluoride (PVDF) membranes (Millipore Co., Ltd, Cat. No. IPVH00010). The PVDF membrane was blocked using 5% skim milk at room temperature for 1 h, followed by incubation with specific primary antibodies against cyclinD1 (diluted at 1: 1000; Abcam, Cat. No. ab137867), MMP-9 (diluted at 1: 1000; Genetex, Cat. No. GTX108624), HuR (diluted at 1: 1000; Abcam, Cat. No. ab238528) and GAPDH (1: 10000; Abcam, Cat. No. ab181602) over night at 4℃. After incubation with secondary antibodies labelled with horseradish peroxidase at 37℃ for 1 h, the immunocomplexes were developed with ECL regent (Millipore Co., Ltd, Cat. No. WBKLS0500). Target bands were quantitatively analyzed using the Image J software (BioRad, USA).

RNA Immunoprecipitation (RIP) assay

RIP assay was performed with RNA-binding protein immunoprecipitation kit (Millipore Co., Ltd, Cat. No. 17–701) in HA-VSMCs. Cells were lysed in RIPA lysis buffer. Afterwards, cell lysates were incubated in RIP buffer containing magnetic beads conjugating antibodies against HuR or negative control IgG for 3 h. Subsequently, the beads were washed with lysis buffer. After elution, immune precipitated RNA was extracted with TRIzol reagent, and RT-PCR (forward primer: 5′- GCGGGTCTGTTTCTTTACTTC – 3′; reverse primer: 5′- GTGGT TGTAAAGTGCAGCAT – 3′) was then assessed by agarose gel electrophoresis to prove lncRNA H19 binding to immune-precipitated HuR.

RNA pull-down

RNA pull-down was performed using a Pierce™ Magnetic RNA-Protein Pull-Down kit (Thermo Fisher Scientifific, Cat. No. 20164), and nuclease-free environment was maintained during this experiment. Briefly, cell lysate was prepared with standard immunoprecipitation (IP) lysis buffer (Thermo Fisher Scientifific, Cat. No. 87788). The streptavidin magnetic beads were washed and then combined with the sense and antisense probes of biotin-labeled lncRNA H19. After RNA binding, the lysate was incubated with the beads in protein-RNA binding buffer at 4 ℃. Then, RNA binding protein complexes were eluted and analyzed by western blotting.

Actinomycin D mRNA stability assay

Actinomycin D (5 μg/ml; Sigma-Aldrich, Cat. A9415) was added to culture medium before the measurement of target mRNA stability. Total RNA was isolated at the indicated times (0, 4, 8, and 12 h) and the remaining level of each specific mRNA was determined with qPCR. Nonlinear regression analysis was used to calculate mRNA half-life[24–27].

Statistical analysis

Experimental data were analyzed by GraphPad Prism 6.0 software (GraphPad Software, La Jolla, CA, USA). All data were expressed as mean ± standard deviation (SD). One-way ANOVA analysis was conducted to compare three or more groups of data. If the data followed a Gaussian distribution, then Bonferroni's multiple comparisons were used as a posttest. Otherwise, the nonparametric Kruskal-Wallis test and Dann's multiple comparison posttest were used to analyze the data. he Student's *t*-test was used for pairwise comparisons between groups. All the experiments were independently conducted at least three times. Differences were considered statistically significant when $P < 0.05$.

Gene	Forward primer (5'–3')	Reverse primer (5'–3')
lncRNA H19	GCGGGTCTGTTTCTTTACTTC	GTGGTTGTAAAGTGCAGCAT
cyclin D1	CCCGCACGATTTCATTGAAC	AGGGCGGATTGGAAATGAAC
MMP-9	GAAAGCCTATTTCTGCCAGG	TGCAGGATGTCATAGGTCAC

Table 1. Primers used for qPCR.

Results

ICA promoted LncRNA H19 expression in ox-LDL-induced HA-VSMCs

Based on microarray analysis in previous work[10], lncRNA H19 (Gene ID: NR_001592) was identified the top 10 upregulated lncRNAs upon ICA intervention (Supplementary Table S1). Therefore, qPCR was performed to validate of the microarray data. The result showed similar trends to that observed in the microarray assay. In detail, the expression of lncRNA H19 was down-regulated in aorta of model group compared with control group, whereas lncRNA H19 was up-regulated in ICA-treated compared with model groups (Fig. 1A-B). Our recent research has indicated that ox-LDL significantly induces cell proliferation and migration at 25 μg/ml in HA-VSMCs. Moreover, ICA shows the inhibitory effect on cell proliferation and migration in HA-VSMCs, 10 μM is the most efficient concentration of ICA [11]. Accordingly, 10 μM ICA was utilized to explore the functions of key molecules in this work. We then observed that the expression of lncRNA H19 was markedly decreased in HA-VSMCs stimulated using ox-LDL. However, ICA increased the expression of lncRNA H19 in HA-VSMCs exposed to ox-LDL (Fig. 1C).

Given that the up-regulated expression of lncRNA H19 was associated with the action of ICA, we performed a collection of gain-of-function experiments to explore whether lncRNA H19 could regulate the function of HA-VSMCs in the progression of AS in vitro. We primarily constructed siRNAs against H19 and plasmid vector expressing full-length H19 to test the efficiency of overexpression or knockdown in HA-VSMCs. The efficiency of overexpression was revealed in Fig. 1D, while si-H19-2 directed to the most effective reduction was illustrated in Fig. 1E.

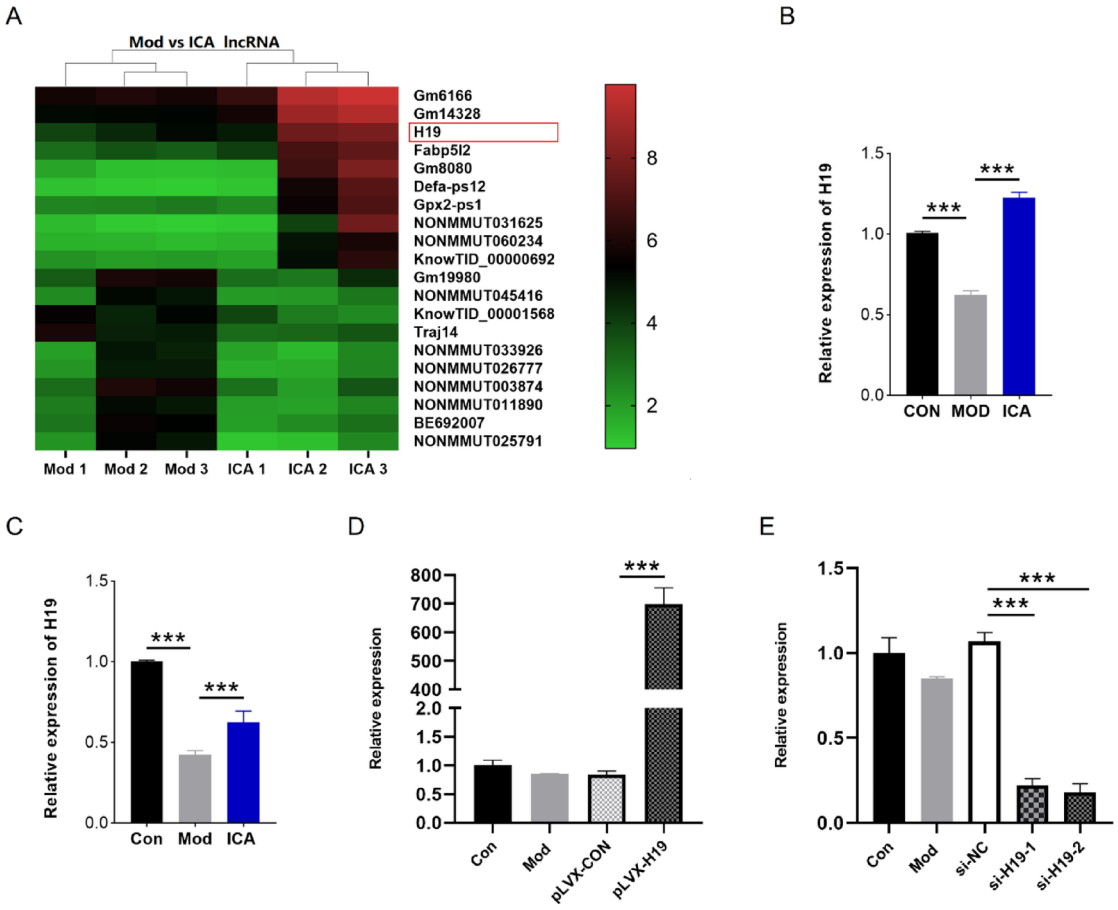

Fig. 1. ICA can regulate the expression of lncRNA H19. (**A**) Heat map from microarray of lncRNAs expression related to the top 20 ectopic regulated lncRNAs. (**B**) qPCR analysis showed that lncRNA H19 was down-regulated in aorta of model group compared with control group, whereas lncRNA H19 was up-regulated in ICA-treated group compared with model group. (**C**) Relative expression of lncRNA H19 in ICA-treated HA-VSMCs. (**D**) qPCR showed the expression of lncRNA H19 after transfection with the lncRNA H19-overexpressing vectors. (**E**) qPCR for lncRNA H19 depletion using RNAi in HA-VSMCs. CON: wild type (C57BL/6 J) mice + normal diet + CMC-Na; MOD: ApoE$^{-/-}$ mice + HFD + CMC-Na; ICA: ApoE$^{-/-}$ mice + HFD + ICA 40 mg/kg. CMC-Na: carboxymethylcellulose sodium; HFD: high-fat diet. Con: control group without ox-LDL; Mod: 25 μg/ml ox-LDL; ICA: 25 μg/ml ox-LDL + 10 μM ICA; pLVX-CON: 25 μg/ml ox-LDL + pLVX-IRES-Neo control; pLVX-H19: 25 μg/ml ox-LDL + pLVX-IRES-Neo-H19; si-NC: 25 μg/ml ox-LDL + siRNA control; si-H19: 25 μg/ml ox-LDL + si-H19. ***$p < 0.001$. Data are expressed as means ± SD ($n = 3$).

The effect of LncRNA H19 on proliferation and migration of HA-VSMCs

Meanwhile, we investigated whether lncRNA H19 played a role in ox-LDL-induced proliferation and migration. Initially, we observed that the overexpression of lncRNA H19 significantly reduced cell proliferation compared with model group, whereas the transfection of si-H19-2 resulted in the contrary effect by MTS assay (Fig. 2A). The outcomes were further evaluated with the flow cytometric analysis. As shown in Fig. 2B-C, knockdown of lncRNA H19 promoted cell cycle progression, while overexpression of lncRNA H19 resulted in G0/G1 phase arrest, proposing that lncRNA H19 exerted a negative effect on the G1 to S phase transition. Besides, a transwell assay was conducted to assess the ability of lncRNA H19 involved in ox-LDL-induced migration, and the results indicated that overexpression of lncRNA H19 suppressed the migration capability of HA-VSMCs (Fig. 2D-E). Generally, these observations confirmed that lncRNA H19 could mediate the regulatory effects on ox-LDL-induced proliferation and migration in HA-VSMCs.

Silencing LncRNA H19 reduced the inhibitory effect of ICA on proliferation and migration of HA-VSMCs

To further clarify whether ICA can play a role in cell proliferation and migration through regulating lncRNA H19, we used ICA to treat HA-VSMCs transfected with si-H19-2. MTS assay revealed that knockdown of lncRNA H19 could partially reverse the inhibitory effect of ICA on ox-LDL-induced proliferation (Fig. 3A). Flow cytometric assay suggested that knockdown of lncRNA H19 could partially weaken the hampering effect of ICA on cell cycle progression (Fig. 3B-C). Transwell assay showed that migration ability of HA-VSMCs was significantly elevated in ICA/si-H19-2 group compared with ICA/si-NC group (Fig. 3D-E). These findings showed a critical role for lncRNA H19 as the underlying target of ICA in function of HA-VSMCs.

LncRNA H19 inhibited the expression of cyclin D1/MMP-9 by reducing the stability of cyclin D1/MMP-9 mRNAs

Since our recent study has confirmed that the effect of ICA administration on HA-VSMCs might depend on its negative regulation of cyclin D1 and MMP-9 expression [11], we subsequently focused on the regulatory function of lncRNA H19 in the expression of cyclin D1 and MMP-9. The expression of cyclin D1 and MMP-9 significantly decreased in cells overexpressing lncRNA H19. In contrast, levels of cyclin D1 and MMP-9 were up-regulated in cells with silenced lncRNA H19 expression, indicating that cyclin D1 and MMP-9 are the downstream effectors of lncRNA H19 (Fig. 4A-C). After using actinomycin D to inhibit transcription, the levels of cyclin D1 mRNA and MMP-9 mRNA were detected at different times (4 h, 8 h, 12 h), the expression of cyclin D1 mRNA and MMP-9 mRNA was declined after lncRNA H19 overexpression in HA-VSMCs, suggesting that the mRNA stability of cyclin D1 and MMP-9 was evidently reduced on account of the overexpression of lncRNA H19 (Fig. 4D). Collectively, lncRNA H19 could suppress mRNA stability of cyclin D1 and MMP-9.

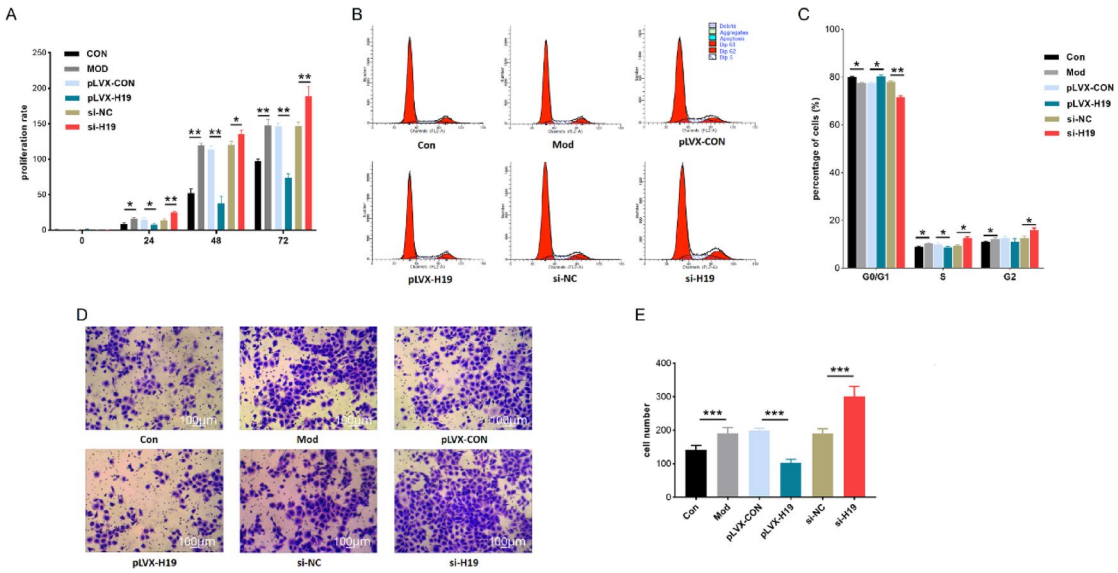

Fig. 2. lncRNA H19 inhibits HA-VSMCs proliferation and migration. **(A)** MTS assays was performed to assess cell proliferation for HA-VSMCs transfected with pLVX-H19 or si-H19. **(B)** and **(C)** Cell-cycle distribution was measured by propidium iodide staining in HA-VSMCs transfected with pLVX-H19 or si-H19, followed by flow cytometric analysis. **(D)** and **(E)** Transwell migration assay for HA-VSMCs transfected with pLVX-H19 or si-H19. Con: control group without ox-LDL; Mod: 25 μg/ml ox-LDL; pLVX-CON: 25 μg/ml ox-LDL + pLVX-IRES-Neo control; pLVX-H19: 25 μg/ml ox-LDL + pLVX-IRES-Neo-H19; si-NC: 25 μg/ml ox-LDL + siRNA control; si-H19: 25 μg/ml ox-LDL + si-H19. $^{*}p < 0.05$; $^{**}p < 0.001$; $^{***}p < 0.001$. Data are expressed as mean ± SD from three independent experiments.

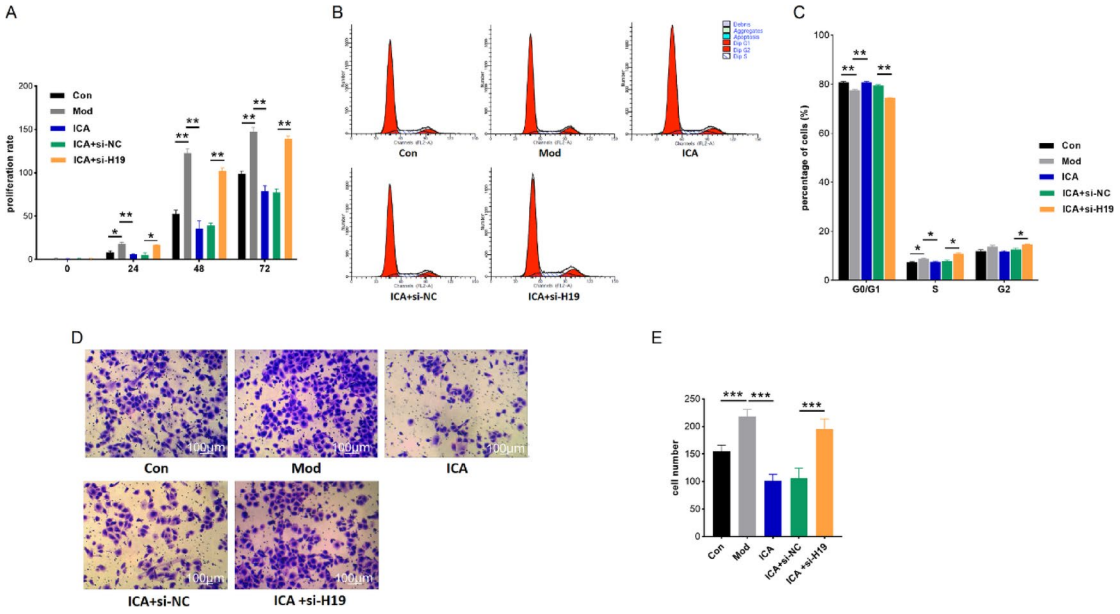

Fig. 3. lncRNA H19 depletion can reverse the inhibitive effects of ICA on proliferation and migration of HA-VSMCs. **(A)** MTS assay was employed to detect cell proliferation after ICA treatment and transfection of si-H19. (**B**) and (**C**) Flow cytometry assay was utilized to detect cell-cycle distribution of HA-VSMCs treated with ICA and transfected with si-H19. **(D)** and **(E)** Transwell assay was conducted to detect cell migration after ICA treatment and transfection of si-H19. Con: control group without ox-LDL; Mod: 25 μg/ml ox-LDL; ICA: 25 μg/ml ox-LDL + 10 μM ICA; ICA + si-NC: 25 μg/ml ox-LDL + 10μM ICA + si-NC; ICA + si-H19: 25 μg/ml ox-LDL + 10μM ICA + si-H19. *$p < 0.05$; **$p < 0.001$; ***$p < 0.001$. Data are expressed as mean ± SD from three independent experiments.

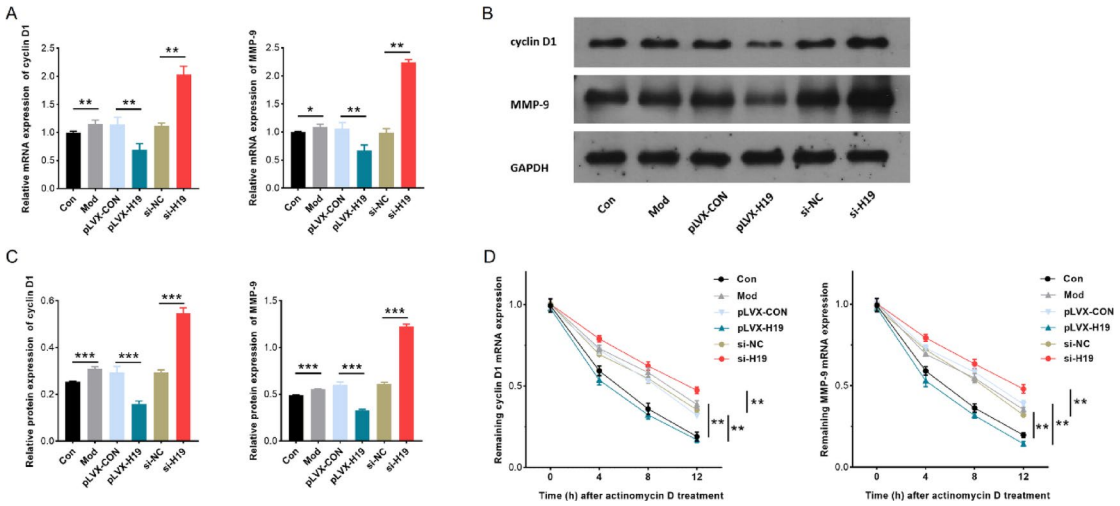

Fig. 4. lncRNA H19 reduces the expression of cyclin D1 and MMP-9 via regulation of target mRNAs stability. **(A)** the levels of cyclin D1 mRNA and MMP-9 mRNA were detected by qPCR after lncRNA H19 overexpression or depletion. **(B)** and **(C)** The protein levels of cyclin D1 and MMP-9 after lncRNA H19 overexpression or depletion were detected by western blot assay. **(D)** the levels of cyclin D1 mRNA and MMP-9 mRNA were examined at different times after administration of actinomycin D. *$p < 0.05$; **$p < 0.001$; ***$p < 0.001$. Data are expressed as mean ± SD from three independent experiments.

The interaction between lncRNA H19 and HuR influence the ability of HuR to bind target mRNAs

Since lncRNA H19 knockdown increased the expression of the well-described target mRNAs (cyclin D1 and MMP-9) of HuR, we demonstrated the interaction between HuR and lncRNA H19 by RIP analysis using anti-HuR and control IgG antibodies, after extracting RNA from the IP samples, qPCR analysis were utilized to estimate lncRNA H19 levels, and normalized to GAPDH mRNA levels in each IP sample. LncRNA H19 was observed to

be substantially enriched by HuR antibody compared with control IgG antibody (Fig. 5A-B), indicating that HuR particularly associates with lncRNA H19. Moreover, we performed biotin-labeled RNA pull-down using specific biotin-labeled lncRNA H19 probe synthesized in vitro, bound to streptavidin beads followed by incubation with cell lysate to detect the related proteins. Immunoblotting with anti-HuR antibody indicated that HuR physically associated with lncRNA H19 in HA-VSMCs (Fig. 5C-D). After lncRNA H19 overexpression or suppression, RIP assay was performed and qPCR was used to detect the levels of cyclin D1 mRNA and MMP-9 mRNA in the product pulled down by anti-HuR antibody. More importantly, lncRNA H19 overexpression reduces the binding of HuR to cyclin D1 mRNA and MMP-9 mRNA, whereas the binding of HuR to cyclin D1 mRNA and MMP-9 mRNA in lncRNA H19 knockdown HA-VSMCs was enhanced remarkably (Fig. 5E-F).

ICA regulated the expression of cyclin D1/MMP-9 through LncRNA H19

To investigate the gene regulatory mechanism of ICA mediated by lncRNA H19, we also used ICA to treat HA-VSMCs transfected with si-H19-2. Specifically, knockdown of lncRNA H19 reversed the inhibitory effects of ICA on mRNA and protein expression levels of cyclin D1 and MMP-9 (Fig. 6A-C). Moreover, we found that ICA administration lowered the half-life of cyclin D1 and MMP-9 mRNAs significantly, and lncRNA H19 knockdown inversely increased the mRNA levels (Fig. 6D). Overall, these results uncovered that ICA regulated the expression of lncRNA H19, which subsequently inhibited the production of cyclin D1/MMP-9.

Discussion

ICA was considered to be effective on AS. Published evidence has shown that ICA functions via multiple pathways including inhibition of high-density lipoprotein (HDL) oxidation and glycation[28], improvement of eNOS/NO-pathway[29], downregulating CX3 C chemokine receptor 1 (CX3 CR1) in macrophage[30], and inhibition of p38 MAPK signaling pathway[31]. Despite its recognized coding target genes, the potential non-coding target genes need to be identified for ICA in AS. Previous evidence has proposed that the anti-atherosclerotic effect of ICA was reversed by miR-205-5p silencing[32]. In the present study, we identified that ICA could regulate the expression of lncRNA H19, which would aid in revealing the efficacy and mechanism of ICA on AS therapy.

The association of lncRNA H19 polymorphisms with the risk of cardiovascular diseases has been indicated[33]. Consistently, dysregulation of lncRNA H19 has been reported in cardiovascular diseases. A recent report has linked lncRNA H19 to AS, wherein lncRNA H19 overexpression was associated with the alleviation of autophagy and mineralization in VSMCs[14]. It has also been clarified that lncRNA H19 was downregulated in ox-LDL induced Raw 264.7 cells, and its depletion increased inflammatory responses and pyroptosis[15]. Moreover, the significant role of lncRNA H19 in proliferation and apoptosis of HA-VSMCs has been unveiled. Overexpression of lncRNA H19 resulted in enhanced apoptosis and decreased proliferation of HA-VSMCs in a time-dependent manner, knockdown of lncRNA H19 inhibited HA-VSMCs apoptosis, whereas no significant effect on the proliferation rate could be observed[34]. Therefore, in AS, the regulatory function of lncRNA H19 has yet to be

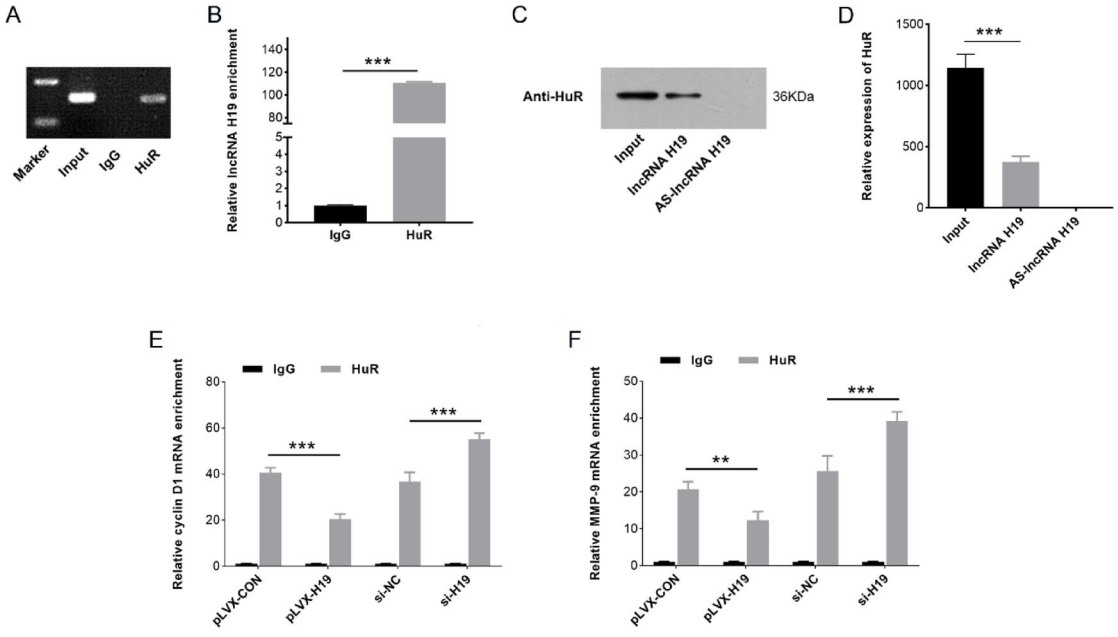

Fig. 5. Competitive binding of lncRNA H19 and target mRNAs to HuR affects HuR binding to target mRNAs. **(A)** and **(B)** RIP and qPCR assays were performed to explore the binding efficiency of lncRNA H19 to HuR protein in HA-VSMCs. **(C)** and **(D)** RNA pull-down and Western blot assays detected the enrichment of HuR in the pull-down of sense lncRNA H19 and anti-sense lncRNA H19. **(E)** and **(F)** Detection of target mRNAs enrichment (cyclin D1 and MMP-9) by qPCR after lncRNA H19 overexpression or knockdown. $^{**}p < 0.001$; $^{***}p < 0.001$. Data are expressed as mean ± SD from three independent experiments.

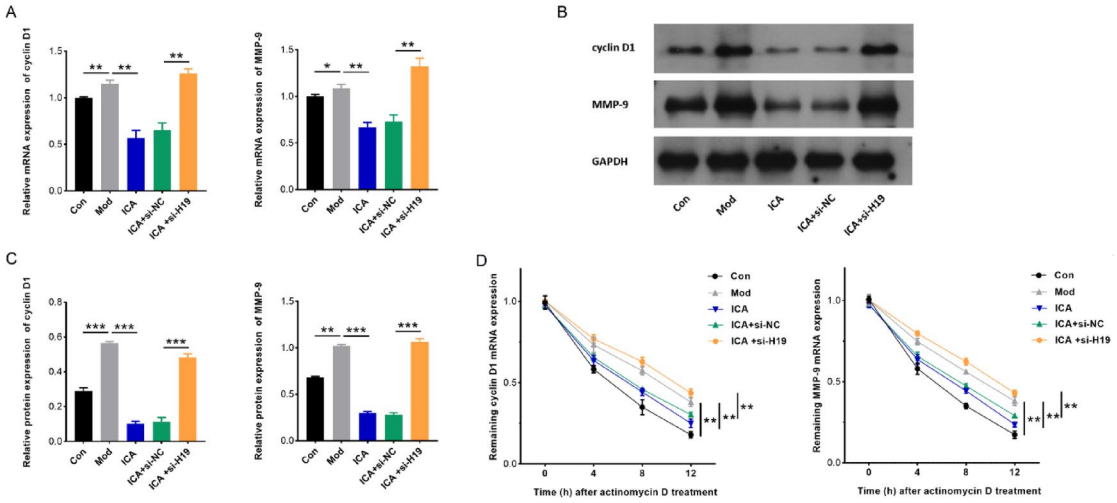

Fig. 6. ICA regulates the expression of cyclin D1 and MMP-9 via lncRNA H19. **(A)** qPCR was utilized to measure the mRNA levels of cyclin D1 and MMP-9 in HA-VSMCs treated with ICA and transfected with si-H19. **(B)** and **(C)** Western blot was performed to detect the protein levels of cyclin D1 and MMP-9 in HA-VSMCs after ICA treatment and transfection of si-H19. **(D)** After inhibiting transcription with actinomycin D, the mRNA expression of cyclin D1 and MMP-9 was detected at different times by qPCR. $^{*}p < 0.05$; $^{**}p < 0.001$; $^{***}p < 0.001$. Data are expressed as mean ± SD from three independent experiments.

fully investigated. In this research, gain or loss of function assays verified that excessive lncRNA H19 could inhibit proliferation and migration of HA-VSMCs. Particularly, we substantiated that lncRNA H19 knockdown attenuated the effect of ICA on HA-VSMCs. Furthermore, it was found that lncRNA H19 could regulate the expression of cyclin D1 and MMP-9. Notably, we ulteriorly confirmed that lncRNA H19 directly associated with the stability of cyclin D1/MMP-9 mRNAs.

LncRNA, the effective modulator in transcriptional regulation and post-transcriptional regulation, are capable of serving as a platform and collect relative proteins. Interactions between lncRNAs and RBPs were reported recently and have aroused interest. Besides serving as an independent lncRNA, lncRNA H19 is the primary precursor of miR-675. The interaction between lncRNA H19 and HuR has been proven to inhibit the processing of miR-675 from lncRNA H19 in the Caco-2 human colon carcinoma cells, which decreased miR-675 and suppressed intestinal epithelial barrier dysfunction[20]. In our study, RIP and RNA pull-down assays together highlighted the abundant binding relationship between lncRNA H19 and HuR in HA-VSMCs. LncRNAs usually function as endogenous competing RNAs to disable RBPs, sponging their activity away from target mRNAs[35]. Given that HuR binds to target mRNAs (cyclin D1 and MMP-9), we hypothesized that lncRNA H19–HuR interaction may influence the ability of HuR to bind other target mRNAs[16,17]. In support, we silenced lncRNA H19 in HA-VSMCs and conducted RIP analysis of HuR interaction with cyclin D1/MMP-9 mRNAs, the increased enrichments in HuR–mRNA complexes indicated that silencing lncRNA H19 'freed up' HuR for binding to target mRNAs.

In our recent study, the regulatory effect of ICA on cyclin D1/MMP-9 expression was observed. To test this specific mechanism further, we used ICA to treat HA-VSMCs transfected with si-H19, silencing lncRNA H19 reversed the suppressing effect of ICA on cyclin D1/MMP-9 expression. Systematically, we examined the regulatory effect of ICA on stability of cyclin D1/MMP-9 mRNAs. It was revealed that ICA inhibited the expression of cyclin D1/MMP-9 by reducing the stability of cyclin D1/MMP-9 mRNAs.

Nonetheless, several limitations of this present study must be mentioned. First, we clarified the regulatory role of lncRNA H19 on AS only in vitro, but the analysis on animal model was not conducted, limiting the scope of application of this study. Further verifications and reasonable analyses are still worthwhile to validate the regulatory role of lncRNA H19 and its interaction with HuR in vivo, and the role of lncRNA H19 in the ICA-mediated effect. Second, we observed that the half-life of cyclin D1/MMP-9 mRNAs was significantly prolonged in the absence of lncRNA H19 using actinomycin D. This suggested that lncRNA H19 could indeed decrease the stability of these mRNAs, leading to their faster degradation and reduced protein levels. It would be more credible if we preformed Western blot assay to measure the cyclin D1/MMP-9 protein levels in HA-VSMCs. Third, we forced on only one target which has been identified as the important markers in the G1-phase cell cycle regulation of HA-VSMCs. Cyclins, cyclin dependent kinases (CDKs), and cyclin dependent kinase inhibitors (CKIs) are three main types of molecules related to cell cycle regulation. In the G1/S phase transition, cyclin D and cyclin E are involved. In particular, cyclin D binds specific effector CDK4/CDK6 forming a cyclin/CDK hetero-dimeric complex (CCDK) whose phosphorylation in turn facilitates the progression of cells through the G1/S cell cycle checkpoint. In addition, p21(Cip1) and p27(Kip1), which belong to CKIs, can form a complex to block cyclin E/CDK2 kinase activity. Therefore, the detection of the other gene expression levels besides cyclin D1, such as cyclin E, CDK4, CDK2, CDK6, p21 and p27 is valuable for evaluate cell cycle progression of HA-VSMCs. Forth, zymography is described as simple, sensitive, quantifiable, and functional assay to detect

activities of matrix metalloproteinases (MMPs) in biological samples[36]. The principle of zymographic assay is based on the characteristic that gelatinase can catalyze the degradation of gelatin. Zymography can dynamically analyze the changes of gelatinase in the occurrence and development of inflammation and tumor, which is a valuable tool for early clinical diagnosis, treatment and prognosis[37]. Utilizing zymographic methods will further enhance the inhibitory effect of ICA on MMP-9 expression, which will lead more reliable conclusion of our research. The last point, our study focused only on the mechanism of post-transcriptional regulation on MMP-9 expression, especially the stability of mRNA. On the other hand, MMP-9 expression is regulated by transcription factors, such as NF-kB, AP-1, and SP-1[38,39]. In particular, it has been reported that ICA possesses a protective activity against cardiovascular disease by modulating NF-κB signal pathway[40]. Identifying the regulatory relationship between MMP-9 and NF-κB will be valuable for teasing out more target genes of ICA on AS. Further experiments, such as electrophoretic mobility shift assay (EMSA) will need to be conducted to explore the interaction between transcription factors and promoters.

In summary, our study establishes a mechanism by which lncRNA H19 interacting with HuR regulates VSMCs proliferation and migration, with implications for pathophysiological processes of AS. LncRNA H19 is a critical molecular for AS and potentially is an effective target for AS therapy. These findings verify that ICA administration inhibits atherosclerotic progression, altering the expression of cyclin D1 and MMP-9, in a lncRNA H19/HuR dependent manner.

Data availability

Data is provided within the manuscript or supplementary information files.

Received: 28 October 2024; Accepted: 15 April 2025
Published online: 30 September 2025

References

1. Peter, L. The changing landscape of atherosclerosis. *Nature* **592**, 524–533 (2021).
2. Zhang, P., Wang, W. & Li, M. Circ_0010283/miR-377-3p/cyclin D1 axis is associated with proliferation, apoptosis, migration, and inflammation of oxidized low-density lipoprotein-stimulated vascular smooth muscle cells. *J. Cardiovasc. Pharmacol.* **78**, 437–447 (2021).
3. Yang, H., Mohamed, A. S. & Zhou, S. H. Oxidized low density lipoprotein, stem cells, and atherosclerosis. *Lipids Health Dis.* **11**, 85 (2012).
4. Healy, A. et al. Statins disrupt macrophage Rac1 regulation leading to increased atherosclerotic plaque calcification. *Arterioscler. Thromb. Vasc Biol.* **40**, 714–732 (2020).
5. Zhi, W., Liu, Y., Wang, X. & Zhang, H. Recent advances of traditional Chinese medicine for the prevention and treatment of atherosclerosis. *J. Ethnopharmacol.* **301**, 115749 (2023).
6. Li, R. L. et al. Natural flavonoids derived from herbal medicines are potential anti-atherogenic agents by inhibiting oxidative stress in endothelial cells. *Front. Pharmacol.* **14**, 1141180 (2023).
7. Liu, X., Liu, Z., Miao, Y., Wang, L. & Yin, H. Sex hormone-like effects of Icariin on T-cells immune modulation in spontaneously hypertensive rats. *J. Ethnopharmacol.* **269**, 113717 (2021).
8. Yu, L. M. et al. Icariin attenuates excessive alcohol consumption-induced susceptibility to atrial fibrillation through SIRT3 signaling. *Biochim. Biophys. Acta Mol. Basis Dis.* **1868**, 166483 (2022).
9. Liu, Y. et al. Icariin as an emerging candidate drug for anticancer treatment: current status and perspective. *Biomed. Pharmacother.* **157**, 113991 (2023).
10. Zhang, Y. et al. Effects of Icariin on long noncoding RNA and mRNA expression profile in the aortas of apoE-deficient mice. *Biosci. Rep.* **39**, BSR20190855 (2019).
11. Zhang, Y. et al. Essential role of protein kinase C BI in icariin-mediated protection against atherosclerosis. *J. Pharm. Pharmacol.* **73**, 1169–1179 (2021).
12. Ren, X. et al. Long noncoding RNA TPRG1-AS1 suppresses migration of vascular smooth muscle cells and attenuates atherogenesis via interacting with MYH9 protein. *Arterioscler. Thromb. Vasc Biol.* **42**, 1378–1397 (2022).
13. Jiang, W. et al. SNHG12 regulates biological behaviors of ox-LDL-induced HA-VSMCs through upregulation of SPRY2 and NUB1. *Atherosclerosis* **340**, 1–11 (2022).
14. Song, Z. et al. Association of Astragaloside IV-inhibited autophagy and mineralization in vascular smooth muscle cells with LncRNA H19 and DUSP5-mediated ERK signaling. *Toxicol. Appl. Pharmacol.* **364**, 45–54 (2019).
15. Liu, S. et al. LncRNA H19 mitigates oxidized low-density lipoprotein induced pyroptosis via caspase-1 in Raw 264.7 cells. *Inflammation* **44**, 2407–2418 (2021).
16. Brennan, C. M. & Steitz, J. A. HuR and mRNA stability. *Cell. Mol. Life Sci.* **58**, 266–277 (2001).
17. Lal, A. et al. Concurrent versus individual binding of HuR and AUF1 to common labile target mRNAs. *EMBO J.* **23**, 3092–3102 (2004).
18. Ray, M. et al. Genetic deletion of IL-19 (interleukin-19) exacerbates atherogenesis in $Il19^{-/-}$×$Ldlr^{-/-}$ double knockout mice by dysregulation of mRNA stability protein HuR (human antigen R). *Arterioscler. Thromb. Vasc Biol.* **38**, 1297–1308 (2018).
19. Simion, V. et al. A macrophage-specific LncRNA regulates apoptosis and atherosclerosis by tethering HuR in the nucleus. *Nat. Commun.* **11**, 6135 (2020).
20. Zou, T. et al. H19 long noncoding RNA regulates intestinal epithelial barrier function via MicroRNA 675 by interacting with RNA-binding protein HuR. *Mol. Cell. Biol.* **36**, 1332–1341 (2016).
21. Pang, J. et al. Co-delivery of siAEG-1 and doxorubicin to treat osteosarcoma via nanomicelles for azide-alkyne click conjugation of poly(l-lysine) dendrons onto Zein. *Int. J. Biol. Macromol.* **264**, 130729 (2024).
22. Radmanesh, F. et al. Hydrogel-mediated delivery of microRNA-92a inhibitor polyplex nanoparticles induces localized angiogenesis. *Angiogenesis* **24**, 657–676 (2021).
23. Song, H. et al. CREG1 deficiency impaired myoblast differentiation and skeletal muscle regeneration. *J. Cachexia Sarcopenia Muscle.* **15**, 587–602 (2024).
24. Donahue, J. M. et al. The RNA-binding protein HuR stabilizes survivin mRNA in human oesophageal epithelial cells. *Biochem. J.* **437**, 89–96 (2011).
25. Bai, J. et al. Silencing LncRNA AK136714 reduces endothelial cell damage and inhibits atherosclerosis. *Aging* **13**, 14159–14169 (2021).
26. Feng, J. et al. STAT1 mediated long non-coding RNA LINC00504 influences radio-sensitivity of breast cancer via binding to TAF15 and stabilizing CPEB2 expression. *Cancer Biol. Ther.* **22**, 630–639 (2021).

27. Song, Y., Gao, F., Peng, Y. & Yang, X. Long non-coding RNA DBH-AS1 promotes cancer progression in diffuse large B-cell lymphoma by targeting FN1 via RNA-binding protein BUD13. *Cell. Biol. Int.* **44**, 1331–1340 (2020).
28. Kim, J. Y. & Shim, S. H. Epimedium Koreanum extract and its flavonoids reduced atherosclerotic risk via suppressing modification of human HDL. *Nutrients* **11**, 1110 (2019).
29. Xiao, H. B., Sui, G. G. & Lu, X. Y. Icariin improves eNOS/NO pathway to prohibit the atherogenesis of Apolipoprotein E-null mice. *Can. J. Physiol. Pharmacol.* **95**, 625–633 (2017).
30. Wang, Y., Wang, Y. S., Song, S. L., Liang, H. & Ji, A. G. Icariin inhibits atherosclerosis progress in Apoe null mice by downregulating CX3CR1 in macrophage. *Biochem. Biophys. Res. Commun.* **470**, 845–850 (2016).
31. Hu, Y. et al. Icariin attenuates high-cholesterol diet induced atherosclerosis in rats by Inhibition of inflammatory response and p38 MAPK signaling pathway. *Inflammation* **39**, 228–236 (2016).
32. Huang, P. et al. Icariin alleviates atherosclerosis by regulating the miR-205-5p/ERBB4/AKT signaling pathway. *Int. Immunopharmacol.* **114**, 109611 (2023).
33. Gao, W. et al. Association of polymorphisms in long non-coding RNA H19 with coronary artery disease risk in a Chinese population. *Mutat. Res.* **772**, 15–22 (2015).
34. Li, D. Y. et al. H19 induces abdominal aortic aneurysm development and progression. *Circulation* **138**, 1551–1568 (2018).
35. Kim, J. et al. LncRNA OIP5-AS1/cyrano sponges RNA-binding protein HuR. *Nucleic Acids Res.* **44**, 2378–2392 (2016).
36. Trelford, C. B. et al. LKB1 and STRADα promote epithelial ovarian cancer spheroid cell invasion. *Cancers (Basel).* **16**, 3726 (2024).
37. Kim, H. et al. The ethanol extract of Cyperus exaltatus Var. Iwasakii exhibits cell cycle dysregulation, ERK1/2/p38 MAPK/AKT phosphorylation, and reduced MMP-9-mediated metastatic capacity in prostate cancer models in vitro and in vivo. *Phytomedicine* **114**, 154794 (2023).
38. Jiang, T. et al. Dual role of Baimao-Longdan-Congrong-Fang in inhibiting Staphylococcus aureus virulence factors and regulating TNF-α/TNFR1/NF-κB/MMP9 axis. *Phytomedicine* **139**, 156477 (2025).
39. Zhu, F. et al. $CRL3^{Keap1}$ E3 ligase facilitates ubiquitin-mediated degradation of oncogenic SRX to suppress colorectal cancer progression. *Nat. Commun.* **15**, 10536 (2024).
40. Luo, Z. et al. Impact of Icariin and its derivatives on inflammatory diseases and relevant signaling pathways. *Int. Immunopharmacol.* **108**, 108861 (2022).

Acknowledgements

We sincerely thank for the help provided by all lab personnel in this research.

Author contributions

Conceptualization, YB.Z. and ZM.F.; methodology, M.L.; software, P.H.; validation, YB.Z., ZM.F. and M.L.; formal analysis, P.H.; investigation, P.H.; resources, P.H.; data curation, M.L.; writing—original draft preparation, YB.Z.; writing—review and editing, ZM.F.; visualization, ZM.F.; supervision, YB.Z.; project administration, YB.Z.; funding acquisition, YB.Z.

Funding

This study was supported by the Natural Science Foundation of Science and Technology Department of Jilin Province (YDZJ202201ZYTS105).

Declarations

Competing interests

The authors declare no competing interests.

Ethics statement

This study was approved by the ethics committee of School of Pharmacy, Jilin University (approval no.20160023). All methods were carried out in accordance with relevant guidelines and regulations. The study was performed in accordance with ARRIVE guidelines.

Declaration of competing interest

The authors have stated that there is no conflict of interest associated with the publication and no financial support, which could have influenced the outcome.

Additional information

Supplementary Information The online version contains supplementary material available at https://doi.org/10.1038/s41598-025-98803-5.

Correspondence and requests for materials should be addressed to Z.F.